Structural, Optical and Thermal Properties of PVA / KI Based Solid Polymer Electrolyte

M.I. Mohammed, A.M. Ismail*, and G.F. Salem

Physics Department, Faculty of Education, Ain Shams University, Roxy, Cairo 11757, Egypt

Solid polymer electrolyte films of polyvinyl alcohol (PVA) doped with different amounts of potassium iodide (KI) were prepared using solution cast technique. Formation of complex structure between PVA polymer and KI salt was confirmed by Fourier transform infrared (FTIR) spectroscopy. The changes of crystallization nature and transition temperatures of the solid polymer electrolyte films were investigated by X-ray diffraction (XRD) and differential scanning calorimetry (DSC). The optical absorption spectra in the wavelength range from 200 to 800 nm were measured and analyzed in terms of absorption formula for non-crystalline materials. The optical band gap energy, refractive index, and dielectric constants were investigated and showed a clear dependence on the KI content. The optical band gap (both direct and indirect) was determined and explained on the bases of incorporation of charge transfer complexes by the dopants. The calculated values of refractive index and the dielectric constants of the solid polymer electrolyte films increased with increasing KI content.

1. Introduction

In the recent years, researches on the electrical and optical properties of polymers have enticed much interesting in view of their applications in electronic and optical devices. Electrical conduction in polymers was studied to understand the nature of the charge transport prevalent in these materials while the optical properties are aimed to realize better reflection, antireflection, interference and polarization properties [1]. In this paper, We have utilized PVA as a host polymer because PVA is semi-crystalline polymer, good charge storage capacity, having high dielectric strength, flexible light weight materials and can be produced at low cost [2, 3]. Various composite materials have been lately synthesized by beginning from different polymers and a wide variety of dopants like oxides, metals, inorganic salts and other particles. The integration of the dopants into polar organic polymers can encourage pronounced changes in various properties of polymers in order to modulate and benefit its properties [4-7]. The studies on potassium ion conducting polymers are scarcely. Less

effort has been made on solid polymer electrolytes based on potassium complex systems. Using potassium electrolytes have several characteristics over their widely used lithium analogues, because potassium is less expensive than lithium and much more numerous. The softness of potassium metal makes it easier to obtain and preserve contact to other components in the electrochemical devices. Further, potassium is less moisture resistant than lithium [8-10].

Conducting polymers contain π-electron backbone responsible for their unusual electronic properties such as high electrical conductivity, low energy optical transitions, low ionization potential, and high electron affinity. This extended (π-conjugated) system of the conducting polymers has single and double bonds alternating along the polymer chain [11,12]. The present work aims to investigate the thermal, structural and optical properties of polyvinyl alcohol (PVA) doped with varying concentration of KI.

2. Experimental

2.1. Materials

Polyvinyl alcohol (PVA) from Alpha chemica, India has molecular weight 1,25,000. and 98 % hydrolyzed was used without further purification. Potassium Iodide also was purchased from Oxford Lab Chem, India.

2. 2 Preparation of PVA / KI films

PVA was dissolved in water by using magnetic stirrer. The weight percentages of KI are (0, 2, 4, 6, 10 wt%) were added to mixture and mixed for 30 minutes to obtain more homogenous solution. The casting technique was utilized to prepare film samples of thickness ~0.2 mm.

2. 3. Characterization

In order to investigate the polymer films, Fourier transform infrared (FTIR) spectra of the neat PVA sample and the sample containing 10 wt% KI were recorded using Shimadzu 8201 in the range of 4000 to 400 cm^{-1}. Differential scanning calorimetry (DSC) measurement was carried out at the temperature range from R.T. up to 250 °C by using shimadzu 50, differential scanning analyzer with a heating rate 10°C /min under nitrogen atmosphere. The X-ray diffraction (XRD) patterns of the pure PVA film and the polymer composite films were recorded at room temperature using an X-ray powder diffractometer (Shimadzu XRD 6000) equipped with Cu Kα as radiation source (λ =1.54Å.) in the 2θ (Bragg angles) range($10^{o} \leq 2\theta \leq 80^{o}$) to determine the information about their structure. The measurements of the absorbance A(λ) and transmittance T(λ) were carried out using a double beam spectrophotometer model (type JASCO, V-570, UV–VIS-NIR, Japan) at normal incidence of light in the wavelength range 400–2500 nm. Air was used as

a reference for the transmittance scan. All the measurements were carried out at room temperature. The measurements obtained by this spectrophotometer have a maximum error of about 1%.

3. Results and Discussion

3.1. Fourier Transform Infrared Studies (FTIR)

FTIR spectroscopy has been used to analyze the interactions between atoms or ions in electrolyte systems. These interactions can induce changes in the vibrational modes of the polymer electrolyte. The FTIR spectrum of pure PVA and PVA doped with 10 wt% are shown in Fig. (1). A broad peak was detected around 2924 cm^{-1} related to the symmetric C–H stretching of pure PVA [13]. This peak is found to be shifted to higher wave numbers in the salt-doped sample. The O–H stretching vibration band in pure PVA sample were observed at 3223–3475 cm^{-1} which were assigned to the intramolecular and intermolecular hydroxyl groups [14]. The other absorption peaks observed in the pure PVA spectrum, are 1715 cm^{-1}, 1664 cm^{-1}, 1429 cm^{-1}, 1386 cm^{-1} and 1097 cm^{-1}. These peaks correspond to the CH_2 asymmetric stretching, C=O stretching vibrations, C=C stretching vibrations, C–H bending vibrations, and C–O stretching vibrations, respectively [15]. The observed IR peak assignments pure PVA and PVA doped with 10 wt% KI are listed in Table (1).

Table (1): FTIR peak assignments for pure PVA and PVA doped with 10 wt% KI samples.

Peak assignments	wave numbers (cm^{-1})	
	pure PVA	PVA + 10 wt% KI
C–H stretching	2924	2937
O–H stretching band	3223–3475	3331–3381
CH_2 asymmetric stretching	1715	1722
C=O stretching vibrations	1664	1658
C=C stretching vibrations	1429	1435
C–H bending vibrations	1386	1388
C–O stretching vibrations	1097	1103

The changes in the vibrational frequencies of the above-mentioned peaks in the FTIR spectrum of pure PVA is due to the formation of dative bond between K^+ and the oxygen coordinating sites in PVA. The strong characteristic peak at 3223–3475 cm^{-1} for hydroxyl group is shifted to 3331–3381 cm^{-1} in the salt-doped PVA sample, indicating the reduction of hydroxyl bands in the complex sample [16]. The absorption bands at 1664 cm^{-1} and 1097 cm^{-1} in pure PVA are slightly displaced to 1658 cm^{-1} and 1103 cm^{-1} in the sample containing 10 wt% KI, respectively. This reveals the complexation of KI with PVA matrix.

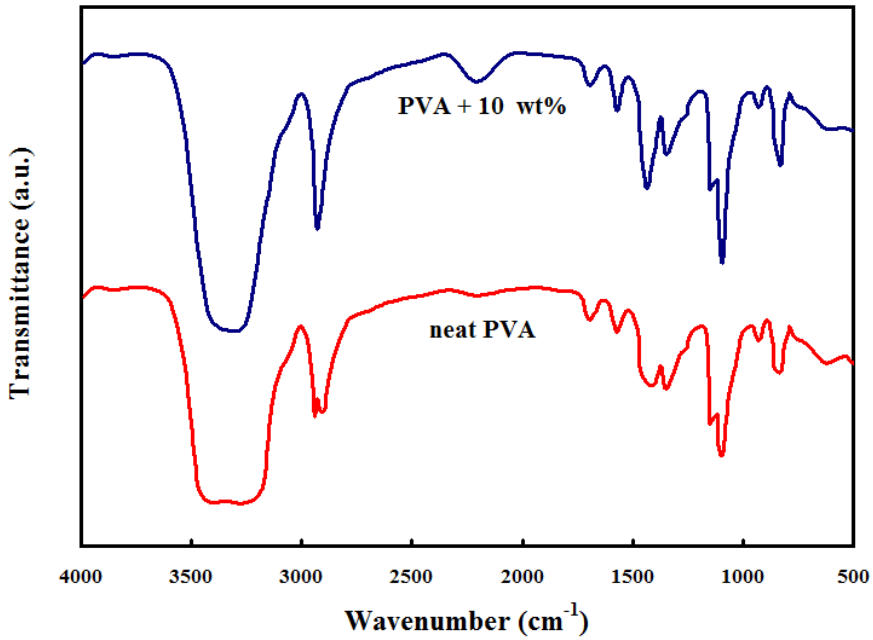

Fig. (1): FTIR spectra of pure PVA and PVA filled with 10 wt% of KI.

3.2. Differential scanning calorimetry (DSC)

Thermal techniques are the suitable tool to define the physical and chemical changes such as phase transitions, glass transition temperatures (T_g) and melting parameters (melting point) T_m, enthalpy of fusion (H_f). The thermal properties of pure PVA and its doped with different concentrations of KI were examined by DSC to appreciate how the thermal transitions of the prepared films were affected by the different concentrations of KI as shown in Fig. (2). The Glass transition (T_g), melting (T_m), melting enthalpies (ΔH_m) and relative crystallinity (X_c%) of pure PVA and PVA filled with different concentrations of KI are listed in Table 2. The observed transitions in the figure can be designated as follows: The exothermic peak (T_w) at about 50 ^{O}C for all the samples could be due to a small amount of moister, which is present in all samples unless it is carefully vacuum dried. Pure PVA curve shows a small endothermic transition (at about 90.9^{O}C) attributed to T_g [17] relaxation process resulting from micro-Brawnian motion of the main chain backbone, a broad transition (centered at about 111.36^{O}C) may be assigned to the α-relaxation associated with the crystalline regions and an endothermic melting peak (T_m) at about 188.91^{O}C. As PVA filled with different concentrations of KI, the melting peak of the composites disappeared for 10wt% due to a large percentage of the filler leading to the weakness in the melting transition. The position of T_g for PVA filled with different filling levels of KI was shifted toward temperatures lower than this of the pure PVA.

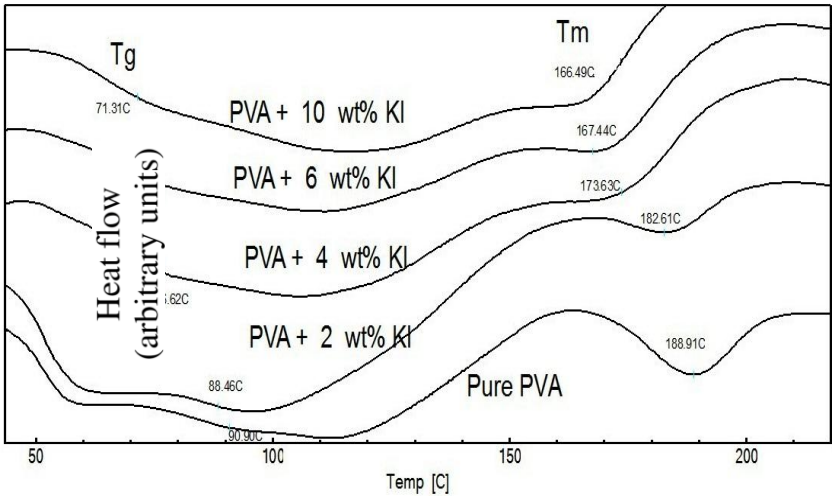

Fig. (2): DSC thermograms of pure PVA and PVA filled with different concentrations of KI.

This suggests that the addition of KI increases the segmental mobility of PVA in and hence, the segments of the filled composites became less rigid. This indicates that the filler acts as plasticizer. By analyzing the thermograms, it is noticed that there is a broadening of the width of α-relaxation which associated with the crystalline region and the enthalpy related with these endothermic decreases with increasing KI content. On the basis of the melting enthalpy, ΔH_m, the degree of crystallinity of pure PVA and the composite films were calculated as follows[18]:

$$X_C = \frac{\Delta H_m}{\Delta H_o X_m} X100 \quad (1)$$

where ΔH_0 is the heat of fusion of 100% crystalline PVA (138.6 J/g) [19] and X_m is the weight fraction of PVA in the composites. The values of T_m, ΔH_m, and X_c% are recorded in Table (2). It is worthwhile to reminder that the deviation in the values of both ΔH_m and X_c% of pure PVA film.[20, 21] can be cleared according to the different synthetic process, physical aging, purity, and average molecular weight of PVA used. Moreover, the crystallinity of the PVA was decreased by the incorporation of KI particles [22, 23].

Table (2): Glass transition (T_g), melting (T_m), thermal decomposition temperatures, melting enthalpies and relative crystallinity of pure PVA and PVA filled with different concentrations of KI.

(wt.%) KI	Glass transition temperature T_g °C	Melting phase transition m T_m °C	ΔH_m(J/g)	X_c%
0	90.9	188.91	20.44	14.74
2	88.46	182.61	7.43	5.4
4	76.62	173.63	5.62	4.22
6	74.85	167.44	4.24	3.25
10	71.31	166.49	4.21	3.37

3.3. X-Ray diffraction analysis

Figure (3) represents the X-ray diffraction of pure PVA and PVA filled with different concentrations of KI as filler. The figure shows in the pure PVA the main peak centered at about $2\theta \approx 20.5^{O}$, and a more peak at 43.9^{O} indicating the semi-crystalline nature of PVA, because it contains crystalline and amorphous structure[24-26]. This diffraction peak confirmed that, obtained polyvinyl alcohol (PVA) is pure without any other impurities. For the filled samples, it is clear that the peak intensity at $2\theta \approx 19^{O}$ decreased and the width of the peak decreased with increase in the concentrations of KI; this is because the interaction between the polymer and the filler leads to decrease in intermolecular interaction between the polymer chains, which implied decrease in the degree of crystallization and hence increase in the amorphous region [27].

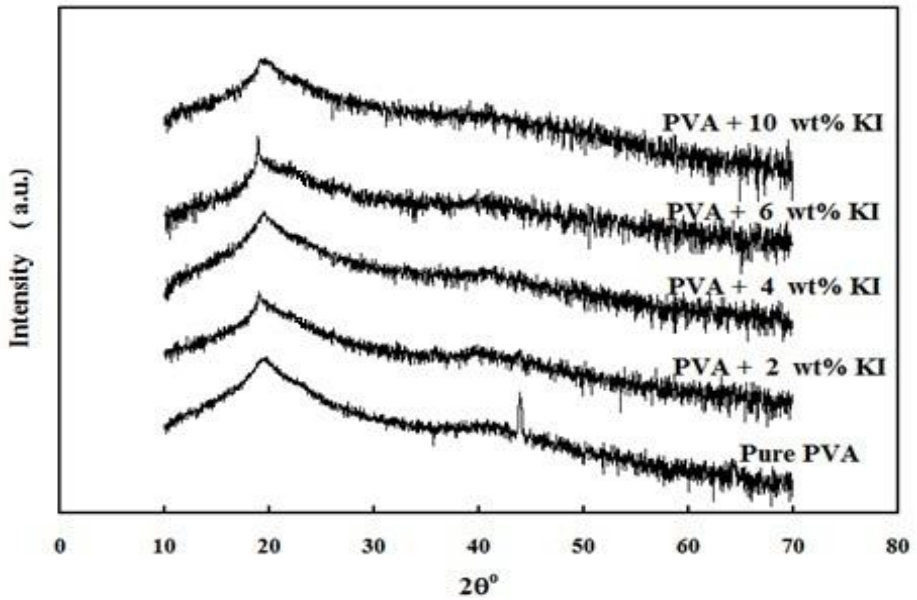

Fig. (3): X-ray diffraction scans of pure PVA and PVA filled with different concentrations of KI.

This behavior demonstrates the complexation between the filler and the polymers blend, which takes place in the polymeric network. [28,29]. No new peaks corresponding to potassium iodide were observed which indicate a complete dissolution of salt in the PVA polymer matrix [30].

3.4. Optical Properties

The optical absorbance as a function of the wavelength of the incident light for pure PVA and PVA -KI composites of various filler contents in the wavelength range of 200–800 nm is shown in figure (4-a). The figure shows that the absorbance increases for filler addition without shift in the peak position. Adding different amounts of filler to PVA polymer does not vary the chemical

structure of the material but leads to create new physical mixture. The observed spectra are characterized by the main absorption edge for all curves and there is no shift in the absorption edge; indicating no clear interaction between PVA matrix and KI. There is one broad absorbance band at about 274 nm [31]. The absorption band may be attributed to change $\pi \rightarrow \pi^*$which comes mainly from unsaturated bonds [32,33]. In general, the absorbance of the films may be of low values in the visible and near infrared region, where at high wavelengths the incident photons may have low enough energy to react with atoms, leading the photons transmitted. When the wavelength decreased, the interaction between incident photon and material will take place, and then the absorbance will rise. In another words, the incident light is absorbed by the free electrons and by increase of the weight percentages of potassium iodide, absorbance is increased.

The variation of transmittance (*T*) as a function of wavelength for pure PVA polymer film and PVA/KI composites is shown in Figure (4-b). Pure PVA is a colorless polymer without any noticeable absorption in the visible range. The pure PVA showed T=63 % and the transmittance increase with increasing concentration of KI. The incorporation of KI inside PVA matrix may act as scattering centers and causes the observed decrease in T% [34], leads to a decrease in light scattering losses.

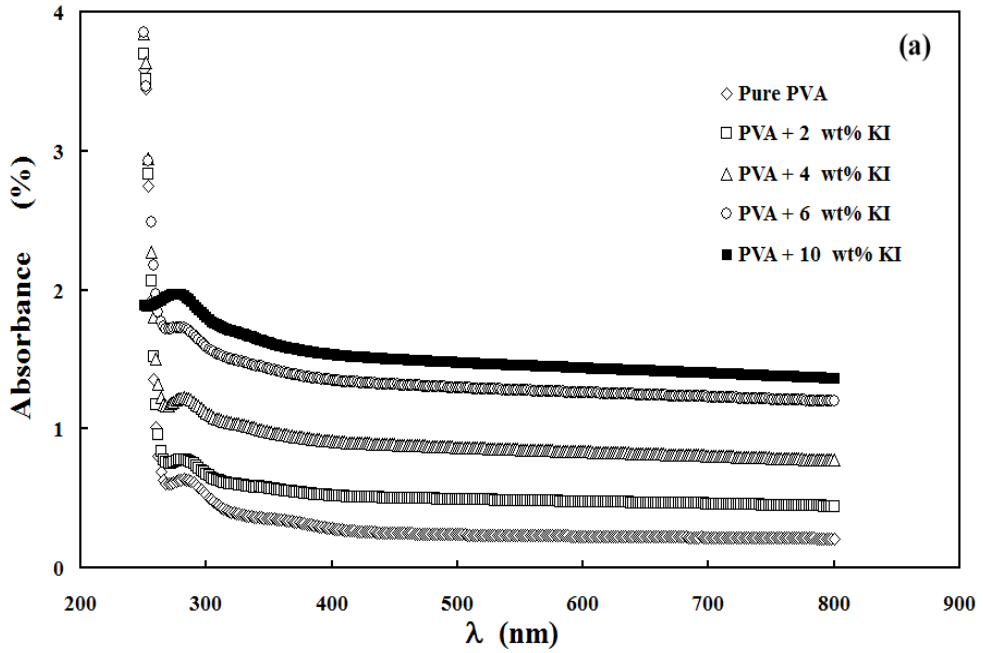

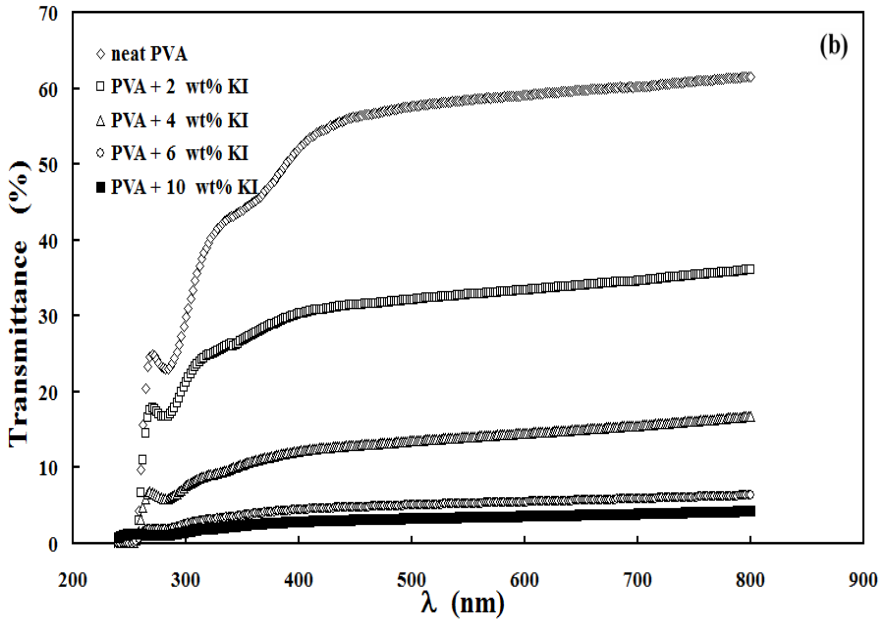

Fig. (4): UV–VIS spectra of pure PVA and the PVA filled with different concentrations of KI.

The optical absorption coefficient (α) of PVA films is very important because it supplies information on the energy gap and electronic band structure, [35]. The absorption coefficient can be calculated as follows:

$$\alpha = 2.303 \frac{A}{d} \qquad (2)$$

where (d) is the thickness of the matter and A is the absorbance .

Figure (5) shows the optical absorption spectrum of composite on photon energy (hν) for different KI concentrations. It was found that the values of ln(α)show a slight increase up to (hν) ≈ 3 eV and then increase at different rates depending on the composite structure. The pure sample had lower absorption coefficient than its composites, this may be due to change in crystallinity due to adding the filler [36]. Analysis of optical absorption spectra could detect the energy gap E_g between the conduction band (CB) and the valence band (VB), according to direct and indirect transitions of both crystalline and amorphous materials.

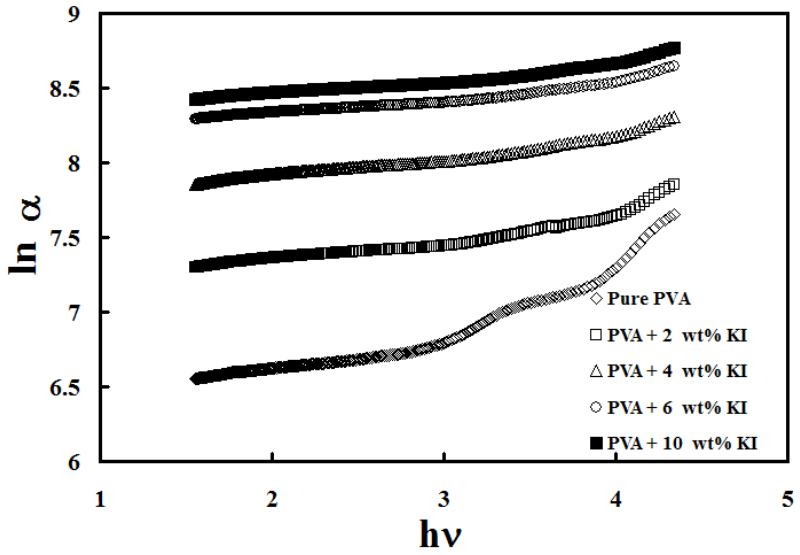

Fig. (5): The absorption coefficient for pure PVA and the PVA filled with different concentrations of KI at various photon energy.

The direct and indirect optical band gaps of the prepared films were investigated using Tuac' relation[37].

$$(\alpha h\nu)^m = B(h\nu - E_g) \quad (3)$$

where hν is the energy of incident photons and m=1/2 for indirect and 2 for direct allowed transitions.[38]

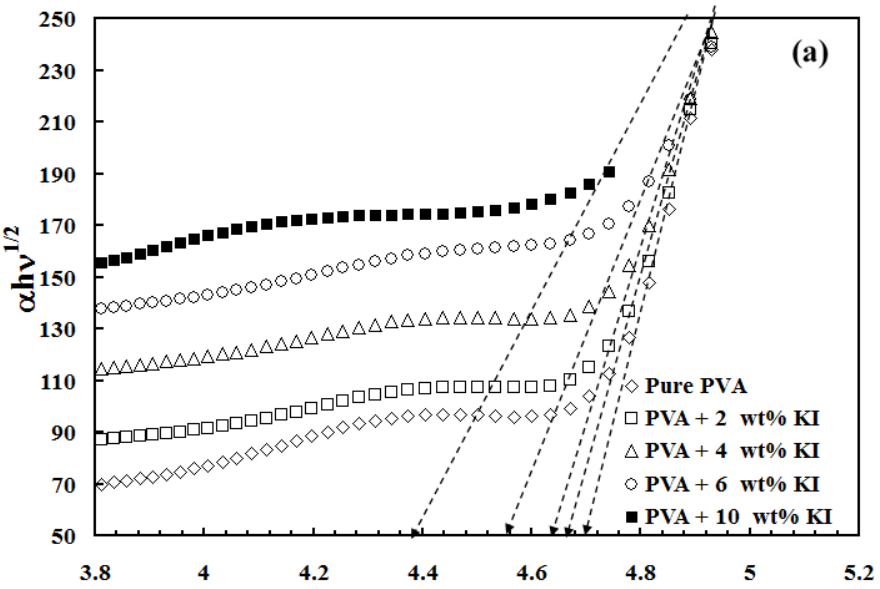

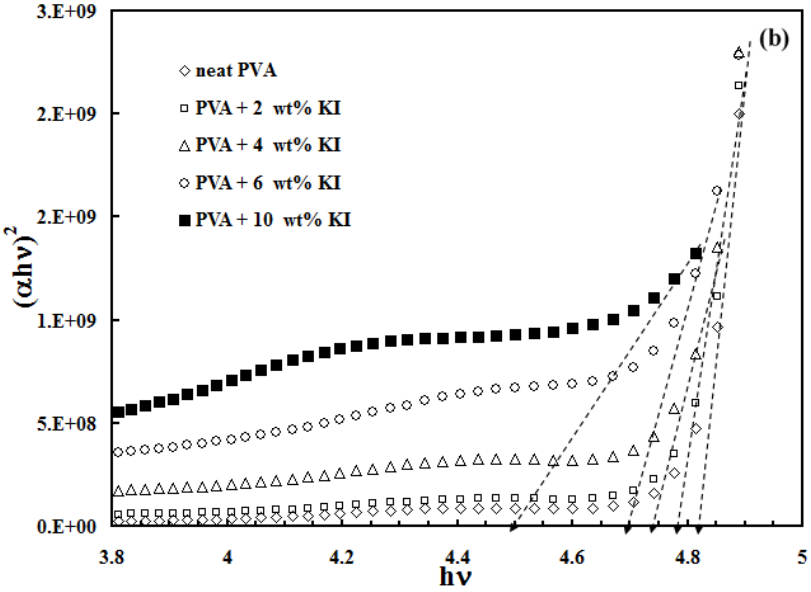

Fig. (6): Plot of $(\alpha h\upsilon)^{0.5}$ and $(\alpha h\nu)^2$ vs. the photon energy ($h\upsilon$) for pure and the PVA filled with different concentrations of KI.

The linear dependence of both $(\alpha h\nu)^{1/2}$and $(\alpha h\nu)^2$ on ($h\nu$) are shown in Fig.6 (a, b). The plots of $(\alpha h\upsilon)^{1/2}$ and $(\alpha h\nu)^2$ versus $h\upsilon$ enable us to appreciate the indirect and direct optical band gap (E_g) by extrapolating the linear part of both $(\alpha h\upsilon)^{1/2}$ and $(\alpha h\nu)^2$ to zero. It is seen from Fig. 6a, that E_g value of the pure PVA sample is 4.68 eV and E_g values show a decrease up to 4.32 eV as given in Table3. From the results obtained it is seen that an increase of concentration of KI in the system leads to decrease in the optical band gap. The decrease in the energy band gap with increasing KI concentration may be attributed to an increase in structural disorder of the polymer films with increasing KI content. Fig. (6.b) shows the relation between absorption edge $(\alpha h\nu)^2$ for PVA and PVA filled with different concentrations of KI. as a function of photon energy ($h\nu$). The obtained values of optical band gap of the composites are recorded in table (2). It is shown that the values of energy gap decrease with increasing KI concentration. This decrease is due to the creation of new levels in the band gap, leading to facilitate the crossing of electrons from the valence band to these local levels to the conduction band. [39,40].

Table. (3): Optical band gap

(wt.%) KI	$E_{g\,(ind)}$	$E_{g\,(dir)}$
0	4.67	4.82
2	4.63	4.77
4	4.59	4.73
6	4.51	4.69
10	4.32	4.49

3.5. Determination of optical constants:

The absorption index (k), refractive index (n) plays a very significant role in optical communication and optical devices. One of the methods for calculating the refractive index (n) is by using the reflectance (R) and the absorption coefficient (k) [41], where $k = \alpha \lambda/4\pi$, λ is the wavelength, α is the absorption coefficient.

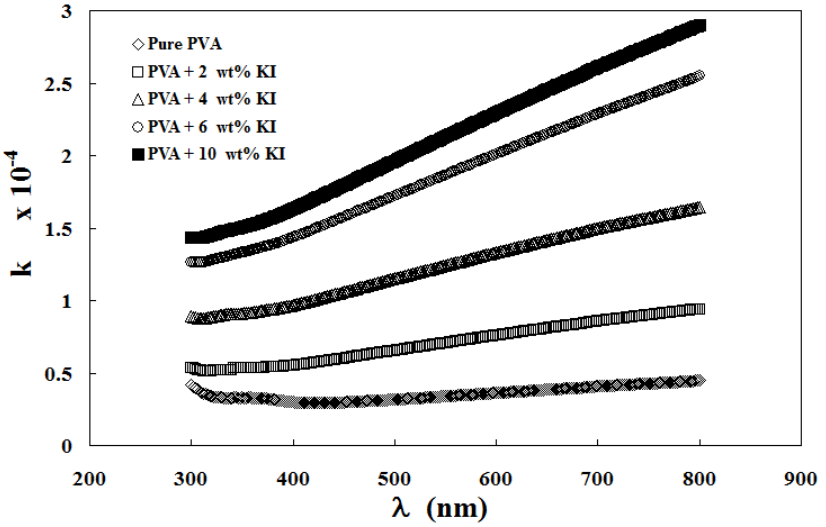

Fig. (7): The Absorption index (k) of pure PVA and PVA filled with different concentrations of KI with wavelength.

Figure (7) shows the dependence of k and absorption spectra of the films on λ. The absorption of pure PVA is lower than that of the filled samples and the absorption increases with increasing KI content in the PVA matrix, this referred to loss of energy because the reaction between the light and the molecules of the medium.

The refractive index as a function of wavelength can be affirmed from the reflection coefficient data R and the absorption coefficient k using equation [42,43]:

$$n = \sqrt{\frac{4R - k^2}{(R-1)^2}} - \frac{(R+1)}{(R-1)} \qquad (4)$$

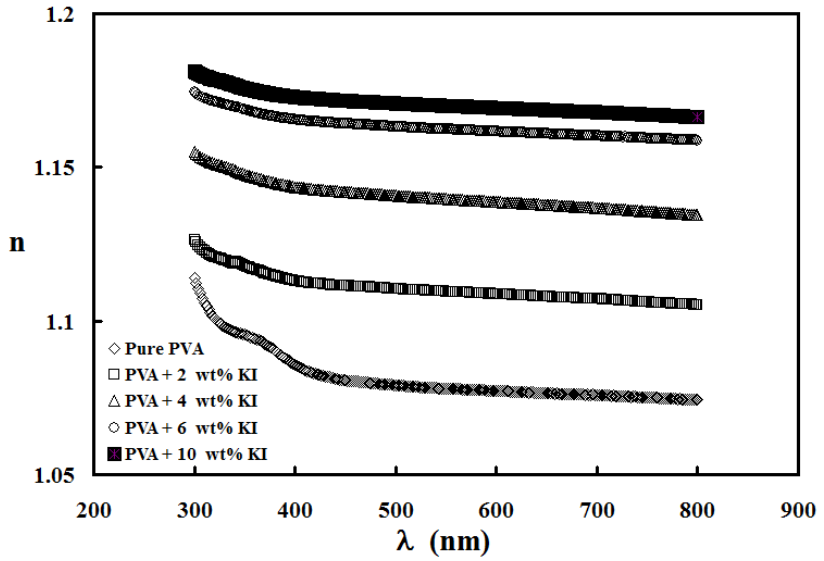

Fig. (8): The refractive index of pure PVA and the PVA filled with different concentrations of KI with wavelength.

Figure (8) shows the refractive index (n) of pure PVA and KI/ PVA composite films as a function of wavelength. The refractive index increases with increasing KI concentration; due to the increased density of the composite films is with doping [44,45].

3.6. Dielectric Constants

The dielectric constant appears the ability of a matter for polarization; the matter can react to different frequencies in a complex manner, at optical frequencies explained by light waves the electronic polarity is dominating above other remaining types of polarization [46].

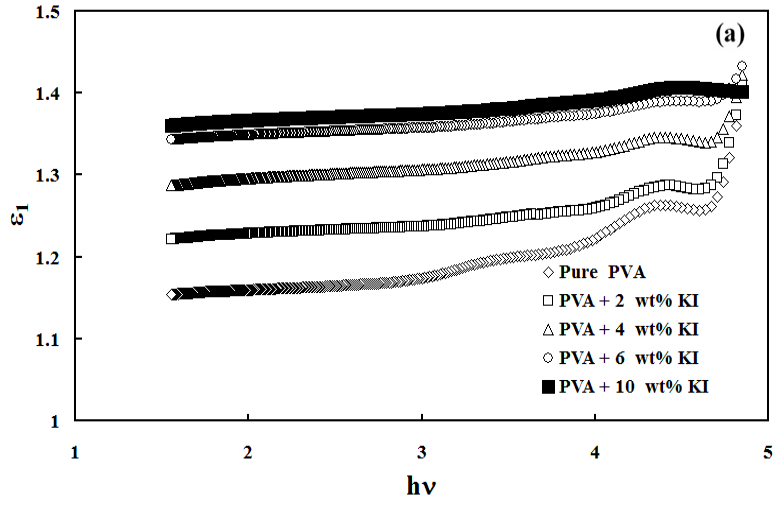

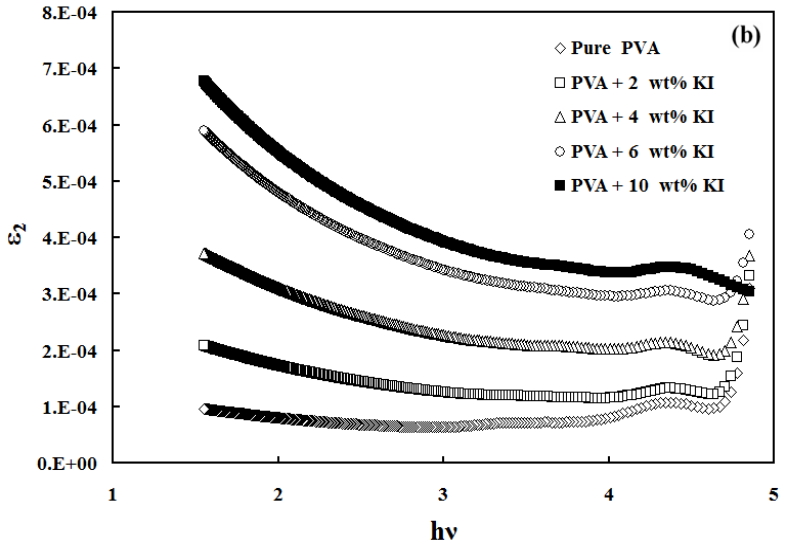

Fig.(9): The dependence of (a) the real, ε_1 and (b) imaginary, ε_2 parts of the optical dielectric constant on hν for pure PVA and the PVA filled with different concentrations of KI.

The real and imaginary dielectric constant can be studied by the following equation

$$\varepsilon_1 = n^2 - k^2 \quad (5)$$

$$\varepsilon_2 = 2nk \quad (6)$$

The real part of dielectric constant is concerned to the dispersion. In order to explain the dispersion it is essentially to take into account the actual motion of the electrons in the optical medium through which the light is traveling. The imaginary part appears the dissipative rate of electromagnetic wave propagation in the medium. The real and imaginary parts reliance on photon energy of samples are shown in Figures 9 (a,b). It can be deduced that ε_1 is larger than ε_2 because it mainly depends on n^2. On increasing the amount of KI in PVA, the real part of dielectric constant increased due to the increase of the dielectric property of films because of KI particles lattice in the host PVA polymer matrix. In the high impurities concentration this may be due to the absence of the resonance between the frequencies of the incident photon energy (electromagnetic and the induced dipoles in the composite [47]. Fig. (9- b) shows the variation the imaginary part of dielectric constant with photon energy. the imaginary part shows how a dielectric soaks up energy from an electric field due to dipole motion, so the variation would be small until it reaches to the high photon energy [48].

4. Conclusions

Polymer films of polyvinyl alcohol with different percentages of potassium iodide have been prepared by casting method. The optical, thermal, structural properties of these composites have been investigated. DSC thermograms revealed that the position of T_g was shifted towards lower temperatures with increasing the filler content, which indicated that the filler acted as a plasticizer. X-ray diffraction scans showed the decrease in the degree of crystallization which caused the increase in the amorphous region. The absorbance of films increases with increasing the concentrations of fillers. The optical constants (absorption coefficient, refractive index and real and imaginary dielectric constants) are increasing with increase of the concentrations of KI. Optical energy band gaps (both direct and indirect) show a decreasing trend with increasing KI concentration as well.

References

1. C. Uma Devi, A.K. Sharma, and V.V.R.N. Rao, *Materials Letters*, **56**, 167 (2002).

2. S.D. Praveena, V. Ravindrachary, R.F. Bhajantri, *Ismayil, Polym Composit*, **27**, 987 (2016).

3. A. Tawansi, A. El-Khodary, and M.M. Abdelnaby, *Current Applied Physics*, **5**, 572 (2005).

4. R.Oslanec, A. C. Costa, R. J. Composto, *Macromolecules*, 33, 5505 (2000).

5. G. Reiter, *Macromolecules*, **27**, 3046 (1994).

6. Adnan KURT, *Turk J Chem*, 34, 67 (2010).

7. A..G.Hadi, F. Lafta, A. Hashim, Hussein Hakim, A. I. O. Al-Zuheiry, S. R. Salman, H. Ahmed, *Universal Journal of Materials Science*, **1**, 52 (2013).

8. T. Sreekanth, M. Jaipal Reddy, S. Subramanyam, U.V. Subba Rao, *Mater. Sci. Eng*. B **64**, 107 (1999).

9. M. Jaipal Reddy, Peter P. Chu, T. Sreekanth, U.V. Subba Rao, *J. Mater. Sci. Mater. Elect*., **12**, 153 (2001).

10. T. Sreekanth, M. Jaipal Reddy, U.V. Subba Rao, *J. Power Sources*, **93**, 268 (2001).

11. R. Nadimicherla, R. Kalla, R. Muchakayala and X. Guo, *Solid State Ionics*, **278**, 260 (2015).

12. M. Jaipal Reddy, Peter P. Chu, *Electrochimica Acta*, **47**, 1189 (2002.

13. Deshmukh K, Ahamed MB, Deshmukh RR, Bhagat PR, Pasha SKK, Bhagat A, Shirbhate R, Telare F, Lakhani C. Polym, *Plast Technol Eng*., 55, 231 (2016).

14. Polua AR, Kumar R. Chinese, *J. Polym Sci*., 31, 641 (2013).

15. Bdewi SF, Abdullah OGh, Aziz BK, Mutar AAR. *J. Inorg Organomet Polym*, 326 (2016).

16. Bhargav PB, Mohan VM, Sharma AK, Rao VVRN. *J. Appl Polym Sci*., **108**, 510 (2008).

17. G. Attia and M.F.H. Abd El-kader Int. *J. Electrochem. Sci*., **8**, 5672 (2013).
18. M. Y. F. Elzayat, S. El-Sayed, H. M. Osman, and M. Amin, *Polym. Eng. Sci*., **52**, 1945 (2012).
19. N. A. Peppas and E. W. Merrill, *J. Appl. Polym. Sci*., **20**, 1457 (1976).
20. R. F. Bhajantri, V. Ravindrachary, A. Harisha, V. Crasta, S. P. Nayak, and *B. Poojary, Polymer*, **47**, 3591 (2006).
21. A. N. Frone, D. M. Panaitescu, D. Donescu, C. I. Spataru, C. Radovici, R.Trusca, and R. Somoghi, *Bio Resources*, **6**, 478 (2011).
22. F. H. Abd El-Kader, W. H. Osman, K. H. Mahmoud, and M. A. F. Basha, *Physica* B **403**, 3473 (2008).
23. A. Hassan, A. M. El Sayed, W. M. Morsi, and S. El-Sayed. *Journal of Applied Physics*, **112**, 3525 (2012),.
24. R.F. Bhajantri, V. Ravindrachary, B. Poojary, Ismayil, A. Harisha, V. Crasta, *Polym Eng Sci*, **49**, 903 (2009).
25. K.S. Hemalatha, K. Rukmani, N. Suriyamurthy, B.M. Nagabhushana, *Materials Research Bulletin*, **51**, 438 (2014).
26. Pal Kunal, Banthia Ajit K., and Majumdar Dipak K., *AAPS Pharm Sci Tech*, **8** (1), 21 (2007).
27. R.M. Hodge, G.H. Edward, G.P. Simon, *Polymer*, **37**, 1371 (1996).
28. H.M. Ragab, *Physica* B **406**, 3759 (2011).
29. R. M. Hodge, G. H. Edward, and G. P. Simon, *Polymer*, vol., **37**, 1371 (1996).
30. O.Gh. Abdullah, *J. Mater Sci: Mater Electron*, **27**, 12106 (2016) .
31. E.M. Abdelrazek, I.S. Elashmawi, *Polym. Comp*. **29**, 1036 (2008)
32. E.M. Abdelrazek, *Physica*, B **403**, 2137 (2008).
33. E.M. Abdelrazek, I.S. Elashmawi, A. El-khodary, A. Yassin. *Current Applied Physics*, **10**, 607 (2010).
34. SG Abd Alla, HM Said, AM El-Naggar, *J. Appl Polym Sci*., **94**, 167 (2004).
35. E.M. Abdelrazek, I.S. Elashmawi, *Polym. Comp*., **29**, 1036 (2008).
36. Tahseen H. Mubarak, *J. Engineering Research and development*, **8**, 15 (2013).
37. J. Tauc, *The Optical properties of solid. North Holland, Amsterdam*, 277 (1972).
38. A. M. El Sayed, H. M. Diab, R. El-Mallawany, *J. Polym Res*., **20**, 255 (2013).
39. E.M. Abdul Razek, A.M. Abdugany, A.H. Oraby, G.M. Asnag, *J. Eng. Technol*., **12**, 98 (2012).
40. Sreetama Dutta, Bichitra N. Ganguly, *J. Nanobiotechnol*., **29**, 10 (2012).
41. S.M. Sze and Ng. Kwok, "*Physics of Semiconductor Devices*", 3rdEd (2006).
42. V. N. Reddy, K.S. Rao , M.C Subha and K. C. Rae, *International Conference on Advances in Polymer Technology, India*, **26**, 356 (2010).
43. R.W.G. Wyckoff, "*Crystal Structures*", Wiley, Vol. 1, New York, (1963).
44. AM El Sayed, WM Morsi, *Polym. Compos*., **34**, 2031 (2013).

45. A. M. El Sayed, S. El-Gamal, W. M. Morsi, Gh. Mohammed. *J. Mater Sci*., **50**, 4717 (2015).
46. A.H. Ahmad, A.M. Awatif and N. Zeid Abdul-Majied, *J. of Eng. & Tech*., **25**, 558 (2007).
47. M.Ghanipour and D. Dorranian, *J. of Nanomaterials*, **2013**, 1 (2013).
48. M. Ali Habeeb1, H. Hakim, and A. Hashim. International. *Journal of Science and Research*, **3**, 10 (2014).